Transient analysis of electrodynamic forces in low-voltage compact busbar

Michał SZULBORSKI [1,4,5] *, Sebastian ŁAPCZYŃSKI [1,6], Paweł SZULBORSKI [1], Łukasz KOLIMAS [1],

Przemysław BEROWSKI [2] and Maciej OWSIŃSKI [3]

[1] Warsaw University of Technology, Faculty of Electrical Engineering, Electrical Power Engineering Institute, 00-662 Warsaw, Poland
[2] Institute of Power Engineering – National Research Institute, High Power Department, 8 Mory St., 01-330 Warsaw, Poland
[3] Institute of Power Engineering – National Research Institute, 8 Mory St., 01-330 Warsaw, Poland
[4] Symkom Sp. z o.o. – ANSYS Channel Partner, ul. Głogowa 24, 02-639 Warsaw, Poland
[5] EARC Innovations, ul. Pana Tadeusza 11/31, 06-100, Pułtusk, Poland
[6] ELKO-BIS Systemy Odgromowe Sp. z o.o., ul. Swojczycka 38e, Wrocław, Poland

Abstract. The paper concerns the effects of electrodynamic forces that act on the current paths of the industrial low-voltage busbar. This work is composed of experimental and simulation sections. In the experimental section, the short circuit tests were presented, and the occurrence of electrodynamic forces was demonstrated. The formation of electrodynamic forces in the current circuits of electrical energy distribution systems is related to the flow of high currents, mostly short circuit currents. To highlight those phenomena a detailed specification of parameters during tests was displayed. In the simulation section, the physical phenomenon of electrodynamic forces is captured by employing a detailed real-scale model of a commercial busbar. Therefore, the authors proposed the employment of the FEA (finite element analysis) to obtain values of electrodynamic forces acting on the current paths by executing a detailed 3D coupled simulation. The analysis of the results and aftermath effects of their interactions led to interesting conclusions that concerned the operation of such power distribution circuits under short-circuit conditions.

Keywords: electrodynamic forces; transient analysis; experimental tests; FEA; busbars.

1. INTRODUCTION

During the development of low-voltage busbar designs, researchers are obliged to determine the electrodynamic load capacity of current tracks. Calculations are made for single- or multi-strip current paths, for example, for busbars of feeder lines in switchgear, current paths connecting sections of switchgear, current paths connecting executive devices in a section of switchgear (circuit breakers, switch disconnectors, and others). In the analyzed cases, calculations of three-pole current path systems become particularly important.

The calculation methods specified in IEC 60865-1:2012 consider cases of current tracks containing simplifications that do not allow precise determination of electrodynamic forces, for example, for a system of current tracks mutually parallel, mutually perpendicular, etc.

All calculations performed to determine the maximum value of electrodynamic interactions for a given current path system require the researcher to know the permissible values of bending stresses and tensile strength of the materials from which the current path is manufactured (copper, aluminium, or a combination in the form of a bimetal of these two metals). Note, however,

that the calculations depend on the accuracy of the material data used for the calculations.

More accurate calculations can be made using numerical coupled analysis, which allows for accurate determination of the values of the interacting electrodynamic forces in single- or multi-strip current paths. After importing a 3D model, which can be a structural model of a given current path from the design, the designer can accurately determine the value of the electrodynamic force in a given system. Coupled analyses can also be performed for various cases:

- The current carrying capacity of a given current path system
- The maximum short-circuit capacity of the current path
- Two-phase and three-phase short circuits
- Different directions of current flow in current paths

2. STATE OF THE ART

The current literature extensively describes the study of electrodynamic force interactions in various devices and current path systems. In [1], the focus shifts to investigating the effect of electrodynamic forces on tulip contact systems in high-voltage circuit breakers, which generally feature two such systems. One tulip system acts as the arcing contact, built from tungsten-coated components that permit thermal expansion. The other system consists of one or two crown contacts, with the arcing system designed as a single, substantial component to maxi-

Bull. Pol. Acad. Sci. Tech. Sci., vol. 73, no. 5, p. e154204, 2025

1

M. Szulborski, S. Łapczyński, P. Szulborski, Ł. Kolimas, P. Berowski, and M. Owsiński

mize surface area, while the crown system is made up of several smaller contacts to enhance contact area and minimize transition resistance. Given the challenges of measuring electrodynamic forces dynamically in the unique conditions within circuit breakers, the authors propose using the finite element method (FEM) for 3D coupled simulations, offering detailed insights into contact system performance under short-circuit conditions.

In the paper [2], the authors conduct analytical calculations for an asymmetric three-phase busbar system, evaluating essential parameters such as the maximum electrodynamic forces, mechanical strength, and the natural frequency of the busbar. These calculations are validated against an ANSYS model of a parallel asymmetric busbar system, confirming the analytical results. The study illustrates that a finite element model is valuable for selecting and optimizing uniquely shaped busbars for various electrotechnical applications, including switchgear.

The study [3] presents a comprehensive analysis of busbar systems under short-circuit conditions, integrating electric, magnetic, thermal, and mechanical factors. Utilizing the finite-element method (FEM), the authors model the interactions among these phenomena. They find that the type of busbar support significantly affects conductor displacement during short-circuit events. While temperature increases from short-circuit currents were assessed, their impact on conductor displacement was minimal. This research underscores the importance of robust support structures in busbar system design to maintain stability and performance during fault conditions.

Reference [4] examines the influence of electrodynamic forces on the current paths in high-grade industrial distribution switchgear. The research includes both experimental and simulation sections, with short-circuit tests demonstrating the forces at work in electrical distribution systems. These forces, triggered by high current flows during short circuits, are meticulously analyzed. The authors employ a real-scale model of the switchgear, advocating the use of the finite element method (FEM) to obtain accurate 3D simulations of the electrodynamic forces, shedding light on how these forces impact system performance under critical conditions.

In the study [5], the authors detail an arrangement of three-phase copper busbars within a low-voltage system, where each phase main conductor is composed of one to four sub-conductors with rectangular cross-sections. They address the hazardous forces posed by short circuits and present three methods for calculating the electrodynamic forces on busbars, culminating in analytical expressions for these forces. By performing calculations on a specific example, the authors demonstrate the effectiveness and precision of each method in predicting electrodynamic forces under short-circuit scenarios.

In the paper [6], the discussion centres on the high electromagnetic forces in low-voltage electromagnetic relays, triggered by fault currents. Such forces can cause contacts to bounce, potentially leading to arc formation and contact welding. To prevent relay failure, it is crucial to determine the threshold for maximum current and electrodynamic force. The study outlines both theoretical calculations and experimental results, identifying the forces and currents at which electrodynamic bounce occurs, thus aiding in the design of contact rivets and relay current paths.

Reference [7] emphasizes the importance of the short-time withstand current (Icw) for air circuit breakers (ACBs), a parameter critical for selective protection. Using a 3D transient finite element method, the study calculates the transient current, repulsion torque, and other dynamic forces affecting ACB stability. The analysis reveals how electromagnetic torque causes phase conductors to tilt and slide under fault conditions, with Phase B exhibiting the weakest stability. The authors propose adding ferromagnet plates to improve dynamic stability, based on both simulation and experimental results.

The paper [8] delves into the emerging modelling approach known as digital twin technology, particularly its application in simulating physical phenomena. The study introduces, validates, and examines a digital twin model tailored to analyze electrodynamic forces in a three-phase high-voltage disconnector. Experimental research and force measurements have revealed considerable difficulties: the investigative process is often complex and expensive and accurately measuring electrodynamic forces under real-world conditions is nearly impossible, even with advanced computational tools. As a result, the researchers utilized sophisticated field models, simplified into reduced order models (ROM), through digital twin technology, offering a promising avenue for progress in this field. Their approach enabled the extraction of results from intricate models, including those required for long-term thermal testing. The digital twin model outcomes were benchmarked and validated against short-circuit test data obtained from laboratory trials.

In the paper [9], the author underscores the crucial role that generator circuit breakers (GCBs) play in electrical power systems. These breakers are designed to withstand extremely high short-circuit currents multiple times during their operational lifetime. Hence, it becomes essential to have an accurate and efficient method to conduct coupled electromagnetic-mechanical simulations of GCBs in their full geometric complexity. The paper proposes a new method for integrating both electromagnetic and mechanical dynamics, allowing for rapid, precise, and efficient simulations of GCBs, especially for complex 3D geometries.

In research [10], the authors investigate how the interrupting performance of low-voltage current-limiting circuit breakers is influenced by the magnitude and distribution of the magnetic field produced by the contact system and splitter plates. To evaluate the impact of different contact system configurations on the current-limiting characteristics, a 3D magnetic field analysis of the arc chamber, including the contact system, arc, and splitter plates, was conducted. Additionally, the electromagnetic repulsion force acting on the movable contact was calculated. The findings are valuable for improving arc chamber designs, and the authors also examined the interaction between the mechanical operating mechanism and the electromagnetic forces.

In the paper [11], the author highlights the importance of the short-time withstand current (Icw) parameter for air circuit breakers (ACBs), as it can lead to electrodynamic stability concerns. This study explores how the closing phase angle and frequency influence the electrodynamic stability of ACBs. By incorporating the skin effect, inter-phase interactions, and the nonlinear B-H characteristics of ferromagnetic materials,

a 3D transient finite element method model for a three-phase ACB was developed. The results indicated that the worst electrodynamic stability for the movable conductors occurs when the closing phase angle (ψ) is equal to $\varphi - \pi/2$, $\varphi + \pi/6$, and $\varphi + 5\pi/6$, where φ denotes the phase angle difference between current and voltage. Moreover, with increasing frequency, peak currents, and repulsion forces shift to a more distributed pattern, while lateral forces acting on conductors adjacent to other phases rise significantly.

In the manuscript [12], the authors explore the interplay between experimental research on three-terminal silicon carbide (SiC) NEMS switches and theoretical analysis to clarify the sources of electrostatic double-layer force (EDF) and the Casimir effect, both of which contribute to stiction. Their findings led to the development of a design aimed at mitigating stiction. They found that finite element modelling and analytical assessments reveal that EDF dominates over the elastic restoring force when the switching gap narrows to a few nanometers, resulting in irreversible stiction upon contact.

In research [13], the authors emphasize the importance of electrical contacts in various electrical devices, including circuit breakers and electromagnetic relays. For long-term reliability, heat distribution during normal operation is a critical factor, as the heat generated correlates with both the current magnitude and the electrical contact resistance. The study utilized numerical simulations with specialized software to analyze heat distribution in electrical contacts, based on actual data from electromagnetic relays.

The manuscript [14] investigates an electrodynamic compensator designed for high-current contacts, featuring a 180-degree bend at the free end of the inactive contact, integrated into the compensator design with contact pads. This alteration reduces the effective shoulder on which the electrodynamic repulsion force acts, thereby decreasing the repulsion moment and simplifying the conditions necessary for full compensation. The paper provides formulas for calculating the additional electrodynamic force associated with the compensator and its contour coefficient, with calculations performed for a rated current of 630 A and a short-time withstand current of 40 kA.

The paper [15] introduces two methodologies, namely, an analytical and a numerical approach, designed to assess electrodynamic forces in switching devices featuring intricate circuit configurations. The analytical method serves as a preliminary design tool, enabling swift evaluation of electrodynamic forces acting on the current-carrying conductors. Conversely, the numerical tool functions as a validation model, assessing forces generated by currents and flux densities using a 3D finite-element method. These methodologies are applied herein to comprehensively analyze an earthing switch tailored for railway applications. Numerical findings are presented to substantiate the efficacy of the proposed methodologies.

In the referenced paper [16], the authors introduce a dynamic analysis method for determining the repulsion forces exerted on current-carrying contacts. This method involves computing the dynamic repulsion forces by integrating the 3-D finite element method (FEM) with magnetic field analysis, current distribution analysis, and motion analysis of contacts. The efficacy of this method was demonstrated through a dynamic analysis of the repulsion forces on contacts.

In reference [17], the focus shifts to investigating the effect of electrodynamic forces on tulip contact systems in high-voltage circuit breakers, which generally feature two such systems. One tulip system acts as the arcing contact, built from tungsten-coated components that permit thermal expansion. The other system consists of one or two crown contacts, with the arcing system designed as a single, substantial component to maximize surface area, while the crown system consists of several smaller contacts to enhance contact area and minimize transition resistance. Given the challenges of measuring electrodynamic forces dynamically in the unique conditions within circuit breakers, the authors propose using the finite element method (FEM) for 3D coupled simulations, offering detailed insights into contact system performance under short-circuit conditions.

In the manuscript [18], the authors create a finite-element model for a stationary contact pair that includes a contact bridge, aimed at analyzing electromagnetic coupled fields. Their simulations focus on how different shape and size parameters of a single-contact bridge influence the electrodynamic force. They also evaluate the effect of the number and spatial distribution of multiple-contact bridges on this force. Findings indicate that in the case of a single bridge, the repulsion force is strongly linked to the perimeter of the contact area. For multiple-contact bridges, the total electrodynamic force is largely affected by the positions of the bridges in the outermost ring. This comprehensive analysis enhances the understanding of how contact geometry impacts electrodynamic forces, which can guide the optimization of contact bridge designs for improved performance.

In the paper [19], the authors investigate dimension-reduction techniques to boost energy efficiency in onboard applications. They assess an earthing switch, an electromechanical device, for its ability to withstand electrodynamic forces. Two methodologies are applied: an analytical approach where electrodynamic forces are estimated based on the assumption of concentrated current flow, and a finite element method (FEM) approach that examines these forces over time. Results indicate that a rectangular cross-section can resist the electrodynamic forces generated by the specified currents. A simple cost analysis shows material savings from redesigning standard earthing knives from a C channel to a rectangular profile, making this study particularly relevant for marine switchgear applications by demonstrating both technical viability and economic advantages.

In the paper [20], the authors introduce an advanced computer modelling technique for analyzing low-voltage extinguishing chambers used in modular devices. The study highlights the phenomenon of enhanced blow-out effects achieved by employing ferromagnetic plates to segment the electric arc within the apparatus. The authors provide a sophisticated tool for investigating the physical phenomena occurring within the extinguishing chamber, enabling analysis of how alterations in component geometry and materials impact current interruption processes. This method is applicable for both alternating current (AC) and direct current (DC) applications, adding significant value for improving the design and performance of various electrical devices.

Bull. Pol. Acad. Sci. Tech. Sci., vol. 73, no. 5, p. e154204, 2025

3

M. Szulborski, S. Łapczyński, P. Szulborski, Ł. Kolimas, P. Berowski, and M. Owsiński

The research in [21] utilizes a 3D finite element method to simulate the transient thermal behaviour of substation connectors. This multiphysics approach includes simulations of both the connectors and the associated power conductors. Validation against experimental data confirms that the finite element method accurately predicts transient and steady-state temperature profiles for both conductors and connectors. Experimental validation involved short-circuit tests conducted in two high-current laboratories. The findings illustrate that this modelling technique is precise and effective for assessing the thermal behaviour of substation connectors. This simulation tool is particularly beneficial during the design and optimization phases, as it can forecast the results of mandatory laboratory tests, thereby enhancing the design process and overall efficiency.

3. THEORETICAL PART

The three-pole single-strip fixed current busbar system is one of the most common solutions in low-voltage busbar designs for currents up to 1600 A. The number of current paths depends on the particular network system in which the busbar is installed. The single-strip three-pole system with parallel arrangement of current tracks is the most typical solution in practice. Performed calculations for this configuration are conducted for the case of a three-phase short-circuit, in which, as can be calculated from the following formula, the highest electrodynamic force occurs at the middle current path, as in

$$F_{2m} = \frac{\mu_0}{4\pi} k_F k_D \frac{\sqrt{3}}{2} \left(i_{ud}^{III} \right)^2, \tag{1}$$

where
k_F – coefficient of formation of two current paths in the form of rail strings arranged in relation to each other,
k_D – Dwight coefficient,
i_{ud}^{III} – surge current for the analyzed case of a three-phase short circuit.

A simplified formula for the electrodynamic force for the centre rail at Dwight's factor $k_D \frac{\sqrt{3}}{2} \approx 1$ can be written as

$$F_{2\max} = \frac{\mu_0}{4\pi} k_F \left(i_{ud}^{III} \right)^2. \tag{2}$$

To perform calculations for a two-phase short circuit for the designed current path, the electrodynamic force vectors in the two current paths are directed opposite to each other. The value of the electrodynamic force can then be determined from the formula

$$F_{\max} = \frac{\mu_0}{4\pi} k_F k_D \frac{\sqrt{3}}{2} \left(i_{ud}^{II} \right)^2, \tag{3}$$

where
i_{ud}^{II} – surge current for the analyzed case of a two-phase short circuit.
However, for calculations for a single-phase short circuit, the value of the electrodynamic force in the current path is

determined from the formula

$$F_{2m} = \frac{\mu_0}{4\pi} k_F k_D \frac{\sqrt{3}}{2} \left(i_{ud}^{I} \right)^2, \tag{4}$$

where
k_F' – current path shaping factor for single-phase short circuit calculations,
i_{ud}^{I} – surge current for the analyzed case of a single-phase short circuit.

As a result of electrodynamic forces, the bending moment applied to the current rail in question is calculated for a beam restrained on both sides. The force in this case is distributed uniformly along the analyzed current path. The bending moment can be calculated from the following formula:

$$M_g = \frac{1}{12} F_m l_1. \tag{5}$$

Conversely, the bending stresses for the analyzed current path can be determined from the following equation:

$$\sigma_g = v_\sigma k_\sigma \frac{M_g}{W}, \tag{6}$$

where
v_σ – dynamic coefficient read from the graph,
k_σ – bending strength coefficient of rails of a given section read from the table.

For the calculations, it is necessary to determine the value of the dynamic coefficient from the graph on bending stresses v_σ for electrodynamic interactions in the case of AC currents calculations performed. The graph is shown in Fig. 1 below.
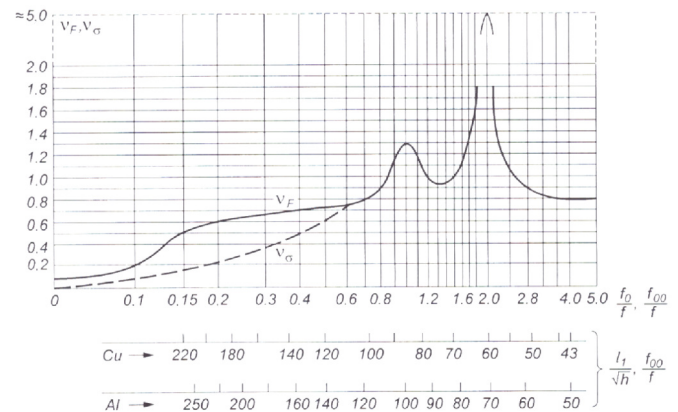

Fig. 1. Chart of values of dynamic coefficients for bending stresses and support reaction forces for electrodynamic forces when performing AC calculations
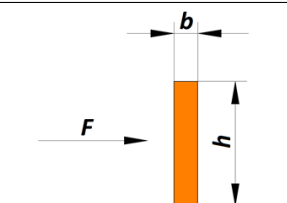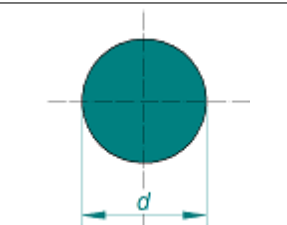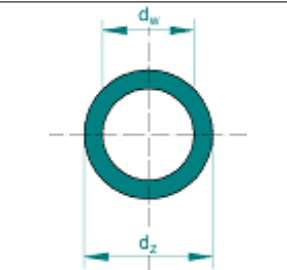
The bending strength coefficients necessary for calculations of rectangular and circular current paths are shown in the following Table 1.

The results of electrodynamic force calculations performed for various cases of short circuits in single-strip current paths are approximate values subject to errors related to inaccurate readings and approximate values taken for calculations. The calculation data obtained are generally not very precise.

4

Bull. Pol. Acad. Sci. Tech. Sci., vol. 73, no. 5, p. e154204, 2025

Table 1

The bending strength coefficients

Cross-section and layout of the current path	Coefficient of strength
F ... b, h (rectangular, force along h)	$W = \dfrac{bh^2}{6} \approx 0.167bh^2$
b ... F, h (rectangular, force along b)	$W = \dfrac{bh^2}{6} \approx 0.167bh^2$
d (solid circle)	$W = \dfrac{\pi}{32}d^3 \approx 0.1d^3$
d_w, d_z (hollow circle / tube)	$W = \dfrac{\pi}{32}\dfrac{d_z^4 - d_w^4}{d_z} \approx 0.1\dfrac{d_z^4 - d_w^4}{d_z}$

4. SIMULATION PART

During research on the design of busbars, coupled numerical analyses may prove to be an essential tool. Their application allows for calculations on precise 3D construction models, enabling the analysis of electrodynamic phenomena related to the flow of short-circuit currents through the current-carrying conductors of prototyped busbars.

The implementation and use of modern, advanced numerical methods for solving such construction-related problems can accelerate development and deployment processes.

To conduct the simulation work associated with this manuscript, a coupled finite element method (FEM) analysis was performed. This approach enables the examination of interactions between various physical phenomena, such as structural, mechanical, and electromagnetic effects. It achieves this by correlating multiple nodes within a numerical program to meet specific conditions and replicate real-world phenomena in a digital environment, similar to the outcomes observed in experimental studies. The coupled FEM analysis relies on transforming interconnected partial differential equations into a set of independent ordinary differential equations through the modal decomposition method. The module utilized for simulating the physical processes was ANSYS Maxwell 3D. Figure 2 below illustrates the key equations incorporated into the module's solver during the calculations.
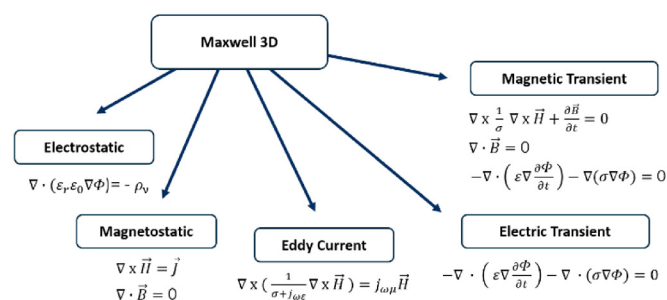
Fig. 2. Functions for analyzing physical phenomena of Maxwell module and mathematical formulas behind them

The choice of Maxwell 3D solver directly influences the calculations, enabling the determination of electrodynamic forces. These calculations are conducted for an applied short-circuit current, with the resulting electrodynamic forces closely tied to the shape of the short-circuit currents within each current path. The boundary conditions were based on one or more of the following magnetic field sources:

- Stranded or solid windings powered by voltage or current
- A permanent magnet

The external boundary conditions were defined as one of the following:

- Default boundary conditions
- Odd symmetry boundary
- Even symmetry boundary

To conduct a coupled analysis of electrodynamic interactions, the authors developed a 3D model of a busbar with a rated current of 1600 A. The model was prepared based on technical data and a physical sample of the KXA 17504-B-STD busbar with a rated current of 1600 A.

The busbar design consists of four current-carrying conductors – L1, L2, L3, and the neutral conductor N. The conductors are insulated from each other using epoxy insulation and are enclosed in a rigid aluminium housing. The developed 3D model is shown in Fig. 3 below.
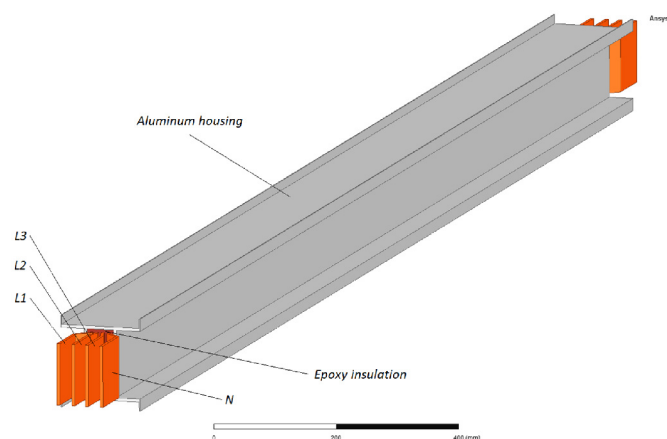
Fig. 3. Developed 3D model of compact busbar design

Bull. Pol. Acad. Sci. Tech. Sci., vol. 73, no. 5, p. e154204, 2025

5

After preparing the 3D model, it was imported into the software solver, where boundary conditions and material properties were applied. In the analyzed busbar, asymmetrical short-circuit currents, including nonperiodic components, were used, which were imported from a .csv file containing data from actual short-circuit tests conducted at IEN. The imported short-circuit current waveforms for the performed simulation are shown in the graph below (Fig. 4).
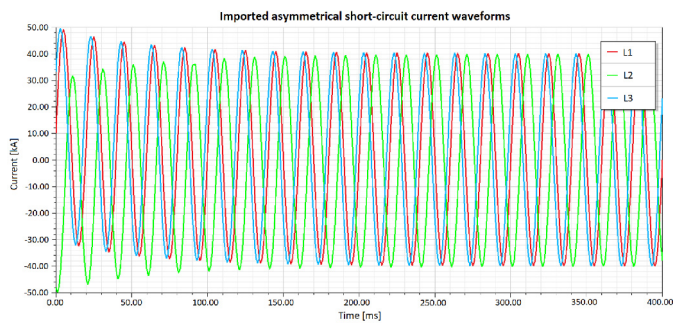

Fig. 4. The imported asymmetrical short-circuit current waveforms with nonperiodic components in phases L1, L2, and L3 from real short-circuit tests conducted at the High-Current Laboratory of the Institute of Power Engineering, Mory, Poland

The flow of asymmetrical short-circuit current through the busbar current-carrying conductors during the computational simulation leads to the generation of eddy currents in the busbar housing, which further intensifies heat generation at the moment of the short circuit.

An example of the electromagnetic induction distribution is shown in Fig. 5 below. From the obtained distribution, it is evident that the highest induction value occurs in the central part of the busbar, reaching 0.6 Tesla along its entire length. This phenomenon is closely related to the density of the short-circuit currents flowing through the three-phase busbar system during the computational simulation. The highest short-circuit current density reached a maximum of $1.0637E^{08}$ A/m^2 in phase L2 at the time of 1 ms in the analysis. This corresponds to the moment when the peak current reached 50 kA, after which, as the nonperiodic component decayed, it began to decrease to 40 kA.
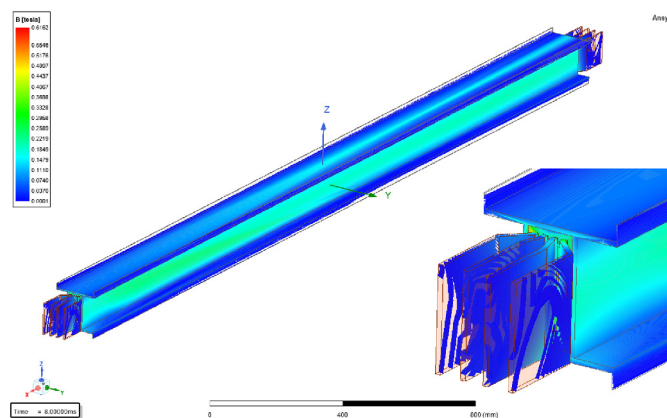

Fig. 5. The distribution of electromagnetic induction in the analyzed busbar

The short-circuit current in the second phase for this simulation step is displaced toward phase L1 due to the interaction with a similarly valued short-circuit current from phase L3 at the same time. Consequently, a higher current density flows in the current-carrying conductor section L2 from the side of phase L1, where the instantaneous value of the short-circuit current is significantly lower. This phenomenon is illustrated in Fig. 6 below, which presents the current density distribution for a simulation time step of 1 ms.
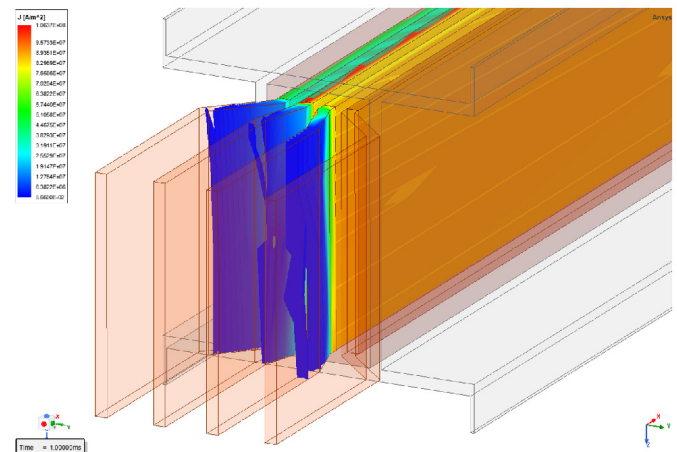

Fig. 6. The distribution of short-circuit current densities in each phase of the analyzed busbar for a simulation time of 1 ms

The results from the simulation for the compact busbar, related to the flow of short-circuit current, allow for the execution of simulations concerning thermal conditions. To perform a thermal analysis related to the heating of the busbar during the occurrence of a short-circuit current, the simulation results from the Maxwell 3D module were imported into the Icepak module for calculations conducted in a "Transient" solver. After loading the "EMLoss" data from the computations in Maxwell 3D, boundary conditions and material properties were applied, similar to the previous module. Additionally, the simulation duration was set to 100 seconds, with each calculation step accompanied by 40 iterative steps. Initial conditions for the ambient temperature were assumed to be at 22°C. The calculations included equations concerning the heat dissipation from the compact busbar through convection and radiation. The results of the calculations are presented below in Fig. 7.

The thermal effects during the flow of short-circuit currents allow for precise determination of how long the insulation between the individual poles of a compact busbar can withstand. It often happens that the busbar can endure the electrodynamic conditions, but the insulation between the busbar current paths becomes damaged.

The thermal analysis clearly shows that the busbar can withstand the high internal temperature for 400 ms, as the temperature rise during this time is negligible, due to the high thermal capacity of the busbar. Temperatures that pose a threat to the busbar insulation occur after approximately 100 seconds, when temperatures exceed 400°C, and can cause insulation damage and generate internal pressure within the busbar. For the as-
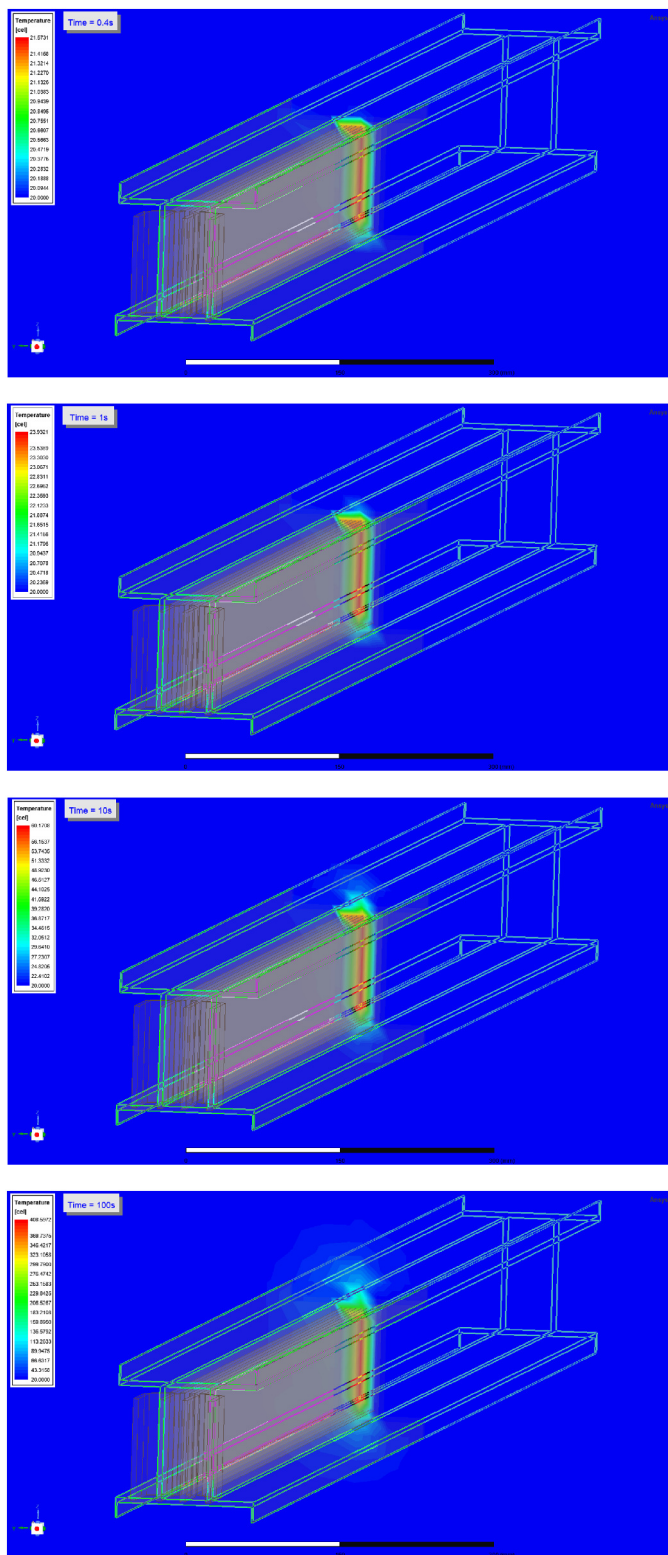
6

Bull. Pol. Acad. Sci. Tech. Sci., vol. 73, no. 5, p. e154204, 2025

Fig. 8. The distribution of electrodynamic force interactions as the vectors in the analyzed compact busbar

Fig. 7. The distribution of electromagnetic induction in the analyzed busbar

sumed electrodynamic impact time of 400 ms, the busbar will not be destroyed by the effects of temperature. Therefore, the next step was to conduct a simulation to assess the electrodynamic loads on the busbar.

For this purpose, calculations performed in the Maxwell 3D module were used to conduct a coupled analysis that allowed for the examination of electrodynamic interactions in the busbar within the Transient Structural module. After importing the results, it was possible to generate the distribution of forces on the individual current paths of the busbar, as shown in the figure below (Fig. 8).

Additionally, it was possible to precisely analyze where the highest values of electrodynamic forces acted on the busbar. Using the "Force Reaction Probe" function, it was possible to generate electrodynamic force plots for virtually any selected point in the computational grid. This function allowed for the generation of plots for the maximum values of electrodynamic forces over a 200 ms period – the duration of the simulation. The plots presented in the figure below (Fig. 9) were generated for all phase current paths of the busbar, i.e., phases L1, L2, and L3. The presented plots show the electrodynamic force values acting in three directions of the XYZ coordinate system, as well as their exact values in kilonewtons. The highest values of electrodynamic forces obtained from numerical calculations were found in the Y direction, meaning forces acting on the sides of the analyzed busbar (Fig. 10).

The analysis of electrodynamic forces also allowed for the examination of the busbar structure in terms of deformations and distortions. The use of the "Total Deformation" postprocessing function facilitated the analysis of the deformations resulting from the electrodynamic forces. The maximum deformations in the aluminium casing structure of the busbar occurred at the midpoint of its length. At the highlighted point below in Fig. 11, the deformation value reached 2.1538 mm at the edge of the casing. The remaining deformation values at the centre of the busbar reached approximately 2 mm.

The deformations in the busbar structure were caused by the stresses resulting from the interaction of electrodynamic forces.

The highest values were recorded at the busbar connections, where the current paths lacked support from the busbar casing (Fig. 12 above). The analysis also revealed the values that occurred at the centre of the busbar casing, where the greatest deformations of the casing were observed. The reduced stress values from the electrodynamic forces ranged from 15 to 20 MPa.
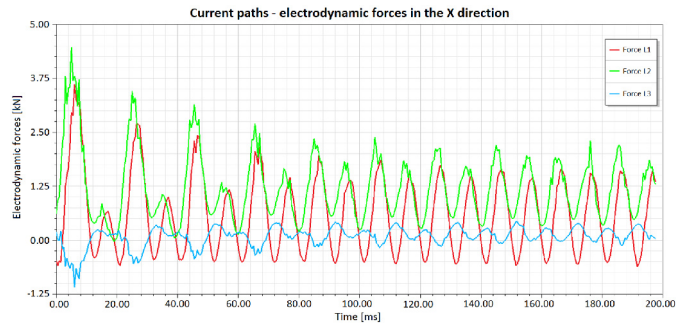
(a) Electrodynamic forces in the X direction for current paths L1, L2, and L3
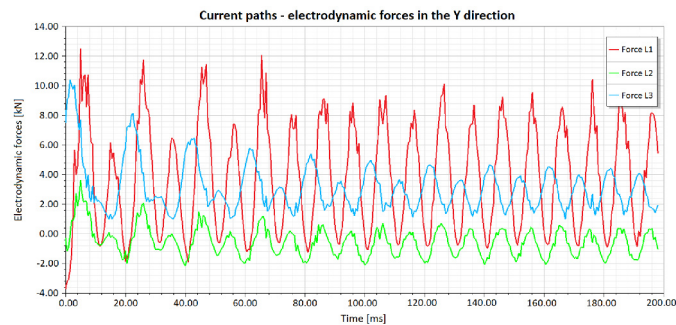
(b) Electrodynamic forces in the Y direction for current paths L1, L2, and L3
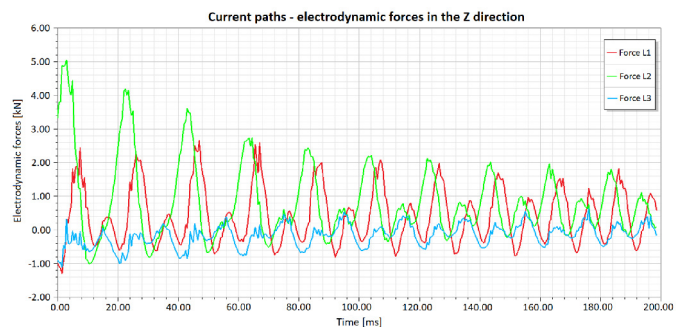
(c) Electrodynamic forces in the Z direction for current paths L1, L2, and L3.

Fig. 9. The electrodynamic force plots obtained from the calculations in the analyzed compact busbar
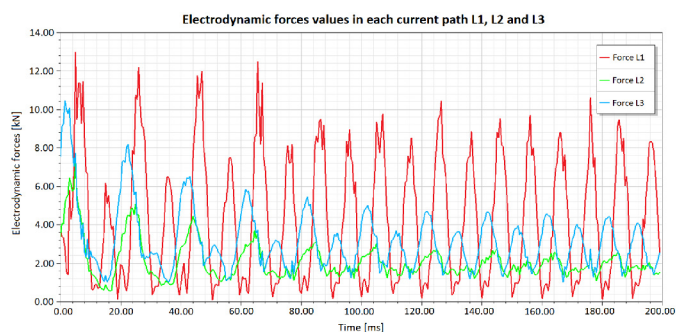

Fig. 10. The plot of maximum resultant electrodynamic forces for current paths L1, L2, and L3 in the analyzed compact busbar
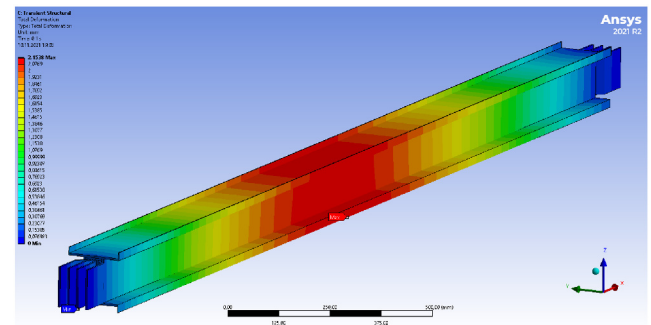

Fig. 11. Maximum deformations in the central part of the analyzed compact busbar
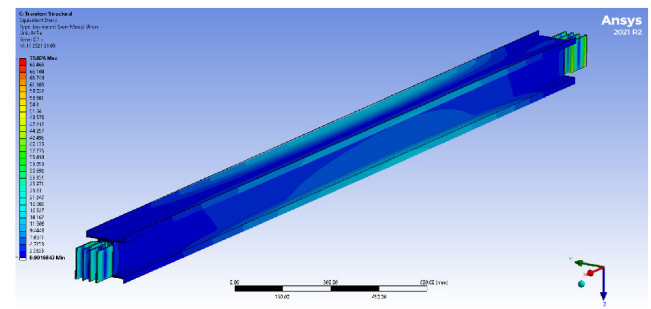

Fig. 12. Maximum stresses resulting from electrodynamic interactions in the analyzed compact busbar

5. LABORATORY TEST RESULTS

In order to conduct short-circuit tests and analyze the effects of electrodynamic interactions, a physical busbar KXA 17504-B-STD with a rated current of 1600 A was delivered to the IEN Large-Current Laboratory in Mory, Poland. The busbar prepared for short-circuit testing is shown in Fig. 13 below.
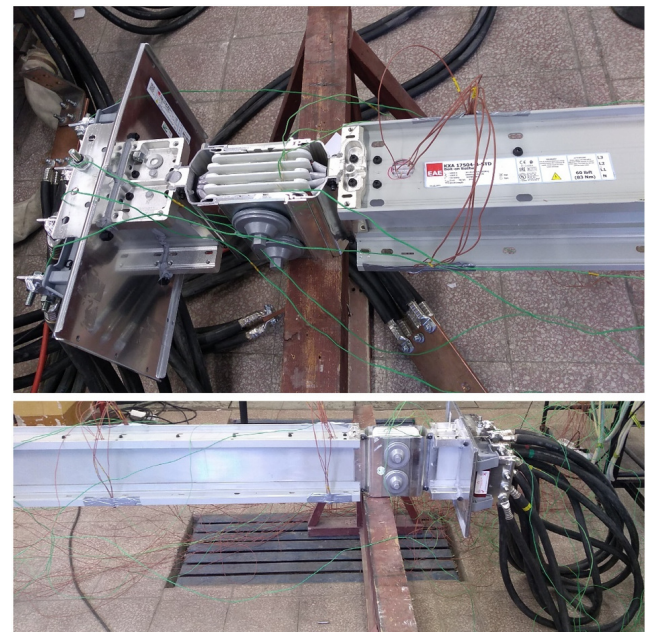

Fig. 13. Tested KXA 17504-B-STD busbar at the Large-Current Laboratory in IEN, Mory, Poland

8

Bull. Pol. Acad. Sci. Tech. Sci., vol. 73, no. 5, p. e154204, 2025

For the short-circuit tests of the busbar system, measurement devices located in the laboratory were utilized. These instruments facilitated precise monitoring and recording of parameters critical for evaluating the electrodynamic forces and thermal effects occurring during the short-circuit conditions. The laboratory setup was specifically configured to ensure the accuracy and repeatability of the experimental results, providing reliable data for analysis and validation of the numerical models.

Short-circuit tests were conducted for a peak short-circuit current equal to 50 kA with the non-periodic component of the short-circuit current. The waveform of short-circuit currents was recorded and saved as a .csv file which was used for simulation analyses.

The highest values were recorded at busbar terminals, where the current paths had no support from the busbar housing. The values of stresses from reduced electrodynamic forces were in the range of 15–20 MPa. These are extremely high values, but during the short-circuit tests in the Large-Current Laboratory, the busbar terminals were not significantly damaged – the terminals were only gently deformed.

6. CONCLUSIONS

The results of the numerical analysis show that a compact busbar of the presented design can withstand the electrodynamic stresses resulting from a three-phase short circuit in which the peak current reaches 50 kA. The results obtained from the calculations are consistent with the results of short-circuit tests conducted at the High Current Laboratory of the Energy Institute in Mory, Poland. During the short-circuit tests, the busbar was not damaged, which confirms the compatibility of the test results with the coupled analysis simulations.

The coupled analysis was shown to be effective in studying physical phenomena in a digital twin 3D model of a compact busbar. Under actual short-circuit test conditions, it is not possible to directly measure the acting electrodynamic forces. It is only possible to analyze their effects, such as deformation and potential damage. Developing a digital twin of the busbar and importing the real short-circuit current waveform for numerical calculations makes it possible to determine the exact values of the electrodynamic forces acting on the current paths.

The authoring team designs and supports the production of modular low-voltage devices, high-current busbars, and distribution equipment. The modelling presented in the study:

- Reduced the design time.
- The 3D time-domain model allows for the analysis of other coupled physical phenomena.
- Electrodynamic forces are measured exclusively in highly constrained systems. Globally, only a few accredited laboratories, following the IEC 60865 standard, attempt to determine electrodynamic forces exclusively for simple flat conductors.
- Electrodynamic forces in the presented structures can practically be measured as an effect rather than directly.

REFERENCES

[1] I.C. Popa and A.-I. Dolan, "Numerical modeling of three-phase busbar systems: Calculation of the thermal field and electrodynamic forces," *2016 International Conference on Applied and Theoretical Electricity (ICATE)*, Craiova, Romania, 2016, pp. 1–9, doi: 10.1109/ICATE.2016.7754608.

[2] M. Szulborski, S. Łapczyński, Ł. Kolimas, Ł. Kozarek, and D.D. Rasolomampionona, "Calculations of Electrodynamic Forces in Three-Phase Asymmetric Busbar System with the Use of FEM," *Energies*, vol. 13, no. 20, p. 5477, doi: 10.3390/en13205477.

[3] G. Kadkhodaei, K. Sheshyekani, and M. Hamzeh, "Coupled electric– magnetic–thermal–mechanical modelling of busbars under shortcircuit conditions," *Generat. Transmiss. Distrib.*, vol. 10, pp. 955–963, 2016, doi: 10.1049/IET-GTD.2015.0706.

[4] S. Łapczyński *et al*., "Electrodynamic Forces in Main Three-Phase Busbar System of Low-Voltage Switchgear – FEA Simulation," *Energies*, vol. 17, p. 1891, 2024, doi: 10.3390/en17081891.

[5] B. Shen, X. Zhang, and D. Zhou, "Analysis and calculation of short-circuit electro-dynamic forces on rectangular bus bars," *2009 IEEE 6th International Power Electronics and Motion Control Conference*, Wuhan, China, 2009, pp. 2618–2621, doi: 10.1109/IPEMC.2009.5157849.

[6] A. Ksiazkiewicz, G. Dombek, K. Nowak, and J. Janiszewski, "Electrodynamic Contact Bounce Induced by Fault Current in Low-Voltage Relays," *Energies*, vol. 12, p. 3926, 2019, doi: 10.3390/en12203926.

[7] J. Qu, Q. Wang, J. Zhang, H. Zhao, G. Wu, and X. Li, "3-D Transient Finite-Element Analysis and Experimental Investigation of Short-Circuit Dynamic Stability for Air Circuit Breaker," *IEEE Trans. Compon. Pack. Manuf. Technol.*, vol. 5, no. 11, pp. 1610–1617, Nov. 2015, doi: 10.1109/TCPMT.2015.2475300.

[8] M. Szulborski *et al*., "Examination of Electrodynamic Forces in High Voltage Disconnector Related to the Short-Circuit Current Using the Digital Twin Technology," *IEEE Access*, vol. 12, pp. 75701–75717, 2024, doi: 10.1109/ACCESS.2024.3404828.

[9] J. Yin, Y. Zhao, Q. Chen, X. Lang, and J. Duan, "3D Magnetic Field Simulation of Generator Circuit Breaker Contact Structure," *2023 International Conference on Power Energy Systems and Applications (ICoPESA)*, Nanjing, China, 2023, pp. 702–706, doi: 10.1109/ICoPESA56898.2023.10140572.

[10] D. Chen, H. Liu, H. Sun, Q. Liu, and J. Zhang, "Effect of magnetic field of arc chamber and operating mechanism on current limiting characteristics of low-voltage circuit breakers," *IEICE Trans. Electron.*, vol. 86, no. 6, pp. 915–920, 2003.

[11] J. Qu, Q. Wang, Z. Liu, H. Zhao, and X. Li, "Influences of Closing Phase Angle and Frequency on Electrodynamic Stability of Air Circuit Breaker," *IEEE Trans. Compon. Pack. Manuf. Technol.*, vol. 6, no. 2, pp. 249–255, Feb. 2016, doi: 10.1109/TCPMT.2015.2511180.

[12] R. Yang, J. Qian, and P. Feng, *Electrodynamic Force, Casimir Effect, and Stiction Mitigation in Silicon Carbide Nanoelectro-mechanical Switches*, Wiley, 2020, doi: 10.1002/smll.202005594.

[13] A. Książkiewicz and R. Batura, "Thermal and electrodynamic characteristics of electrical contacts in steady state," *Poznan Univ. Technol. Acad. J.-Electr. Eng.*, vol. 74, pp. 137–142, 2013.

Bull. Pol. Acad. Sci. Tech. Sci., vol. 73, no. 5, p. e154204, 2025

9

M. Szulborski, S. Łapczyński, P. Szulborski, Ł. Kolimas, P. Berowski, and M. Owsiński

[14] Y.M. Zaitsev *et al.*, "Electrodynamic compensator for high-current contact devices," *IOP Conf. Ser.-Earth Environ. Sci.*, vol. 990, p. 012019, 2022, doi: 10.1088/1755-1315/990/1/012019.

[15] A. Dolara, F. Grimaccia, and S. Zuffetti, "Analysis of Electrodynamic Forces in Switching Devices for Railway Applications," *IEEE Trans. Compon. Pack. Manuf. Technol.*, vol. 7, no. 6, pp. 901–911, June 2017, doi: 10.1109/TCPMT.2017.2687098.

[16] T. Ota, S. Suzuki, and K. Hirata, "Dynamic analysis method of repulsion forces on current - carrying contact using 3-D FEM," *IEEE Trans. Magn.*, vol. 47, no. 5, pp. 942–945, May 2011, doi: 10.1109/TMAG.2010.2091260.

[17] M. Szulborski, S. Łapczyński, Ł. Kolimas, and M. Tyryk, "Electrodynamic Forces in a High Voltage Circuit Breakers With Tulip Contact System—FEM Simulations," *IEEE Access*, vol. 10, pp. 99299–99320, 2022, doi: 10.1109/ACCESS.2022.3207768.

[18] L. Zhou, S. Man, Z. Wang, S. Xue, and W. Ren, "On the Relationship Between Contact a -Spots Features and Electrodynamic Repulsion Force for Electrical Apparatus," *IEEE Trans. Compon. Pack. Manuf. Technol.*, vol. 8, no. 11, pp. 1888–1895, Nov. 2018, doi: 10.1109/TCPMT.2018.2869993.

[19] M. Krčum, M. Zubčić, and T. Dlabač, "Electromechanical analysis of the medium voltage earthing switch due to short-time and peak withstand current test," *Energies*, vol. 12, p. 3189, 2019, doi: 10.3390/en12163189.

[20] M. Szulborski, S. Łapczyński, and Ł. Kolimas, "Increasing Magnetic Blow-Out Force by Using Ferromagnetic Side Plates inside MCB," *Energies*, vol. 15, p. 2776, 2022, doi: 10.3390/en15082776.

[21] F. Capelli, J.R. Riba, and J. Pérez, "Three-Dimensional Finite-Element Analysis of the Short-Time and Peak Withstand Current Tests in Substation Connectors," *Energies*, vol. 9, p. 418, 2016, doi: 10.3390/en9060418.

10

Bull. Pol. Acad. Sci. Tech. Sci., vol. 73, no. 5, p. e154204, 2025